

## Tensor Interaction Limit Derived From the $\alpha$ - $\beta$ - $\bar{\nu}$ Correlation in Trapped ${}^8\text{Li}$ Ions

G. Li,<sup>1,2</sup> R. Segel,<sup>3,2</sup> N. D. Scielzo,<sup>4</sup> P. F. Bertone,<sup>2</sup> F. Buchinger,<sup>1</sup> S. Caldwell,<sup>5,2</sup> A. Chaudhuri,<sup>6,2</sup> J. A. Clark,<sup>2</sup> J. E. Crawford,<sup>1</sup> C. M. Deibel,<sup>7,2</sup> J. Fallis,<sup>6,2</sup> S. Gulick,<sup>1</sup> G. Gwinner,<sup>6</sup> D. Lascar,<sup>3,2</sup> A. F. Levand,<sup>2</sup> M. Pedretti,<sup>4</sup> G. Savard,<sup>5,2</sup> K. S. Sharma,<sup>6</sup> M. G. Sternberg,<sup>5,2</sup> T. Sun,<sup>2</sup> J. Van Schelt,<sup>5,2</sup> R. M. Yee,<sup>8,4</sup> and B. J. Zabransky<sup>2</sup>

<sup>1</sup>Department of Physics, McGill University, Montréal, Québec H3A 2T8, Canada

<sup>2</sup>Physics Division, Argonne National Laboratory, Argonne, Illinois 60439, USA

<sup>3</sup>Department of Physics and Astronomy, Northwestern University, Evanston, Illinois 60208, USA

<sup>4</sup>Physical and Life Sciences Directorate, Lawrence Livermore National Laboratory, Livermore, California 94550, USA

<sup>5</sup>Department of Physics, University of Chicago, Chicago, Illinois 60637, USA

<sup>6</sup>Department of Physics and Astronomy, University of Manitoba, Winnipeg, Manitoba R3T 2N2, Canada

<sup>7</sup>Joint Institute for Nuclear Astrophysics, Michigan State University, East Lansing, Michigan 48824, USA

<sup>8</sup>Department of Nuclear Engineering, University of California, Berkeley, California 94720, USA

(Received 22 October 2012; published 1 March 2013)

A measurement of the  $\alpha$ - $\beta$ - $\bar{\nu}$  angular correlation in the Gamow-Teller decay  ${}^8\text{Li} \rightarrow {}^8\text{Be}^* + \bar{\nu} + \beta$ ,  ${}^8\text{Be}^* \rightarrow \alpha + \alpha$  has been performed using ions confined in a linear Paul trap surrounded by silicon detectors. The energy difference spectrum of the  $\alpha$  particles emitted along and opposite the direction of the  $\beta$  particle is consistent with the standard model prediction and places a limit of 3.1% (95.5% confidence level) on any tensor contribution to the decay. From this result, the amplitude of any tensor component  $C_T$  relative to that of the dominant axial-vector component  $C_A$  of the electroweak interaction is limited to  $|C_T/C_A| < 0.18$  (95.5% confidence level). This experimental approach is facilitated by several favorable features of the  ${}^8\text{Li}$   $\beta$  decay and has different systematic effects than the previous  $\beta$ - $\bar{\nu}$  correlation results for a pure Gamow-Teller transition obtained from studying  ${}^6\text{He}$   $\beta$  decay.

DOI: [10.1103/PhysRevLett.110.092502](https://doi.org/10.1103/PhysRevLett.110.092502)

PACS numbers: 23.40.Bw, 37.10.Mn, 37.10.Ty

Angular correlation measurements in nuclear  $\beta$  decay provide important experimental support [1,2] for the electroweak standard model in which the  $W$  vector boson interacts solely by left-handed vector ( $V$ ) and axial-vector ( $A$ ) interactions with coupling constants  $C_V = C'_V$  and  $C_A = C'_A$  even though five relativistically invariant couplings— $V$ ,  $A$ , scalar ( $S$ ), pseudoscalar ( $P$ ), and tensor ( $T$ ) of either handedness—are possible. However, extensions to the standard model allow  $S$  and  $T$  interactions, e.g., from the exchange of leptoquarks [3]. A global analysis of  $\beta$  decay yields limits on right-handed  $S$  and  $T$  coupling constants  $C_S = -C'_S$  and  $C_T = -C'_T$  of  $|C_S/C_V| < 0.067$  and  $|C_T/C_A| < 0.081$  and limits on left-handed couplings that are over an order of magnitude more stringent at a 95.5% confidence level (C.L.) [2]. A single measurement of the  $\beta$ - $\bar{\nu}$  angular correlation in the  $\beta$  decay of  ${}^6\text{He}$  reported in 1963 [4] (with additional radiative corrections recognized in 1998 [5]) has considerable influence on the  $C_T$  limits. The only other  $\beta$ - $\bar{\nu}$  angular correlation measurement that limits the tensor admixture to significantly less than 10% is a second measurement of the  ${}^6\text{Li}$  recoil spectrum from  ${}^6\text{He}$  decay that reports a 3.1% ( $1\sigma$ ) uncertainty on the  $\beta$ - $\bar{\nu}$  correlation coefficient [6]. In the present work, a result of similar precision on a different nucleus,  ${}^8\text{Li}$ , is obtained by measuring the delayed- $\alpha$  energy spectra.

The use of traps allows  $\beta$ -decay angular correlations to be measured to high precision. Radioactive nuclei can be

held nearly at rest at a known position and the decay products emerge from the trap with minimal interactions, allowing the determination of decay kinematics. Recent measurements of the  $\beta$ - $\bar{\nu}$  angular correlation coefficient performed with atom traps [7,8] and with ion traps [6] have achieved  $\sim 1\%$  precision and several proposed experiments [9,10] are aiming at 0.1% precision.

This Letter reports a search for tensor coupling contributions in the  $\beta$  decay of  ${}^8\text{Li}$ . The  $J^\pi = 2^+$   ${}^8\text{Li}$  ground state decays to the  $2^+$  broad first excited state in  ${}^8\text{Be}$  that immediately breaks up into two  $\alpha$  particles:  ${}^8\text{Li} \rightarrow e^- + \bar{\nu} + 2\alpha + 16.09$  MeV. The transition is predominantly Gamow-Teller [11,12] and *ab initio* calculations have confirmed that the isospin  $I = 1$  component in the  ${}^8\text{Be}$  3.04 MeV state is less than  $10^{-3}$  [13]. Isospin mixing is expected to be very small because the  ${}^8\text{Li}$  ground state is  $I_z = 1$ , which prevents it from having any  $I = 0$  component while in  ${}^8\text{Be}$  the nearest  $J^\pi = 2^+$   $I = 1$  strength is in the 16.6–16.9 MeV doublet. The decay therefore depends only on the  $C_A$  and  $C_T$  coupling constants.

There are several reasons why the decay of  ${}^8\text{Li}$  is particularly attractive for studying  $\beta$ - $\bar{\nu}$  angular correlations. The angular distribution of the  $\bar{\nu}$ 's is determined not only by the  $\beta$ - $\bar{\nu}$  correlation, but also by the angle between the  $\alpha$ 's and the  $\beta$  (as described in detail by Morita [14] and Holstein [15]). This additional correlation arises because the leptons carry away angular momentum and leave the spin of daughter nucleus oriented [16] and, depending on

the choice of the  $\alpha$ - $\beta$  angle, can result in an enhancement (or suppression) of the sensitivity to a tensor admixture. For a  $2^+ \rightarrow 2^+$  Gamow-Teller decay followed by a breakup into two  $0^+$   $\alpha$  particles, when the  $\beta$  and  $\alpha$  particles are detected along the same axis the sensitivity to tensor interactions is enhanced by a factor of 3. Also, the large  $\beta$ -decay  $Q$  value and small nuclear mass leads to recoil energies up to 12.2 keV (at the most probable  ${}^8\text{Be}^*$  excitation energy). The  $\alpha$  particles emitted from the  ${}^8\text{Be}^*$  breakup are in the easily measurable 1.5-MeV range and when emitted along the direction of a 12-keV  ${}^8\text{Be}^*$  recoil differ in energy by 400 keV and when emitted perpendicular to the recoil direction deviate from  $180^\circ$  by  $7^\circ$ . These kinematic shifts are much larger than those in other precision  $\beta$ - $\bar{\nu}$  correlation experiments that have measured the nuclear recoil directly [4,6–8] or have determined the nuclear recoil from delayed-particle emission [17–20].

For an unpolarized sample in the allowed approximation, the  $\beta$ -decay rate is [15,21]

$$W(\theta_{\beta\nu}) \propto F(Z, E_e) p_e E_e (E_0 - E_e)^2 \times \left( g_1 + g_2 \frac{\vec{p}_e \cdot \vec{p}_\nu}{E_e E_\nu} + b \frac{m_e}{E_e} \right), \quad (1)$$

in which  $(E_e, \vec{p}_e)$  and  $(E_\nu, \vec{p}_\nu)$  are the  $\beta$  and  $\bar{\nu}$  four-momenta, respectively,  $E_0$  is the end point energy, and  $F(Z, E_e)$  is the Fermi function. For Gamow-Teller decays, the existing limits on the Fierz interference term  $b$  are  $\sim 0.01$  [22,23], and this term is negligible at the present experimental precision. The ratio  $g_2/g_1$ , typically referred to as the  $\beta$ - $\bar{\nu}$  correlation coefficient  $a_{\beta\nu}$ , is

$$\frac{g_2}{g_1} = \frac{1}{3} \frac{|C_T|^2 - |C_A|^2}{|C_T|^2 + |C_A|^2} = a_{\beta\nu} \quad (2)$$

for a pure Gamow-Teller decay [21]. For a  $\beta$ -decay involving delayed  $\alpha$ -particle emission, as in  ${}^8\text{Li}$  decay, additional correlation terms arise between the leptons and the delayed  $\alpha$  particles, and the decay rate becomes

$$W \propto F(Z, E_e) p_e E_e (E_0 - E_e)^2 \times \left[ g_1 + g_2 \frac{\vec{p}_e \cdot \vec{p}_\nu}{E_e E_\nu} + g_{12} \left( \frac{(\vec{p}_e \cdot \hat{\alpha})(\vec{p}_\nu \cdot \hat{\alpha})}{E_e E_\nu} - \frac{1}{3} \frac{\vec{p}_e \cdot \vec{p}_\nu}{E_e E_\nu} \right) \right], \quad (3)$$

in which  $\hat{\alpha}$  is the unit vector for one of the  $\alpha$  particle momenta, and  $g_{12}$  is defined in Ref. [15] and depends on the spins of the initial, intermediate, and final states as well as the form of the electroweak interaction [14]. For the spin sequence  $2^+ \rightarrow 2^+ \rightarrow 0^+$  in the  ${}^8\text{Li}$  decay,

$$\frac{g_{12}}{g_1} = \frac{|C_T|^2 - |C_A|^2}{|C_T|^2 + |C_A|^2} = 3 \frac{g_2}{g_1}. \quad (4)$$

Therefore, combining Eqs. (1)–(4), when the  $\beta$  and  $\alpha$  particles are detected along the same axis, the angular distribution of the neutrinos relative to this axis is nearly

$W(\theta_{\beta\nu}) \propto 1 + (\vec{p}_e \cdot \vec{p}_\nu)/(E_e E_\nu)$  for a pure tensor interaction and  $W(\theta_{\beta\nu}) \propto 1 - (\vec{p}_e \cdot \vec{p}_\nu)/(E_e E_\nu)$  for an axial-vector interaction.

At recoil order, a number of additional correlations involving the  $\alpha$ -particle momentum also contribute to Eq. (3) and the  $g_1$ ,  $g_2$ , and  $g_{12}$  terms receive an  $E_e$  dependence due to recoil-order and radiative corrections. These corrections can be relatively large due to the large decay  $Q$  value and small nuclear mass [15]. Many of these terms are proportional to the weak magnetism form factor  $b_M$  and the induced tensor form factor  $g_{II}$ . For  ${}^8\text{Li}$ ,  $b_M$  has been measured to be  $60 \pm 1.6$  [24], a result that is consistent with the prediction of the conserved-vector-current hypothesis [24,25]. The induced tensor term is expected to be zero due to the absence of second-class currents [25], and a recent experimental limit in the  $A = 8$  system is  $g_{II}/g_A = -0.28 \pm 0.32$  [26], and thus can be neglected here.

${}^8\text{Li}$  ions were produced using the  ${}^7\text{Li}(d, p){}^8\text{Li}$  stripping reaction. A 24-MeV  ${}^7\text{Li}$  beam provided by the Argonne Tandem-Linac Accelerator System (ATLAS) traversed a cryogenic  $\text{D}_2$  gas target and the reaction products were focused by a large solenoid into a gas catcher [27]. The ion injection system, which is described in detail in Ref. [28], was used to thermalize, collect, bunch, and transport the ions to the Beta-decay Paul Trap (BPT) [29] where the measurements were performed. Just before injection into the BPT, the ions were held in a gas-filled Penning trap [30] where contaminants were removed. The  ${}^8\text{Li}$  ions were injected into the BPT every 100 ms and ejected out of the trap every 5 sec.

The BPT is a linear Paul trap consisting of four sets of segmented planar electrodes (Fig. 1). The ideal (for trapping) hyperbolic electrode structure is replaced by flat plates to enable the detectors to subtend a large solid angle.

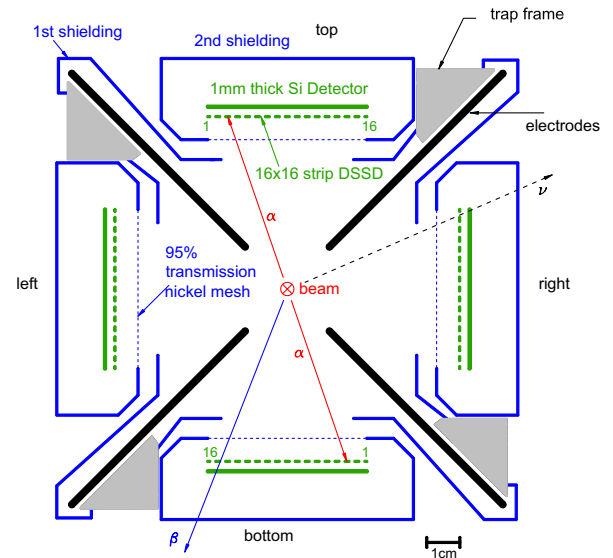


FIG. 1 (color online). Cross-section view of the BPT and detector array.

Along the axial direction of the trap, ions were confined by dc potentials (60, -50, 60 V) applied on the three segments of each electrode. In the radial direction, the ions were confined by the radio frequency (rf) voltage (with a peak-to-peak voltage of 850 V and a frequency of 2.01 MHz) applied to the two pairs of opposite electrodes. The BPT was filled with high purity  $^4\text{He}$  buffer gas at a pressure of about  $1 \times 10^{-5}$  torr to reduce the energy spread of the  $^8\text{Li}$  ions. The trap and detectors were cooled to  $\sim 90$  K by circulating liquid nitrogen inside the electrode support frame. The cryogenic cooling significantly increases the trap lifetime and reduces the thermal energy and spatial spread of the trapped ions. A more detailed description of the BPT is in Ref. [29].

The BPT was surrounded by four sets of silicon detectors each containing a position-sensitive  $50 \times 50 \times 0.30$  mm<sup>3</sup> double-sided silicon strip detector (DSSD) with 16 strips on each side, backed by a  $50 \times 50 \times 1.00$  mm<sup>3</sup> single-element silicon detector (SD). Considerable attention went to ensuring that the performance of the silicon detectors was minimally affected by the rf fields of the trap. The detectors were surrounded by two layers of aluminum casing with independent grounds to minimize the pickup from the rf trapping field. The residual pickup was further suppressed by passing the detector signals through a low-pass filter and by optimizing the time constants of the signal-processing electronics, with the result that there was no significant broadening of the detectors' off-line approximately 50-keV energy resolution. The window of the innermost casing was covered by a 95%-transmission nickel mesh, which was the only solid material between the trap center and the detectors. The DSSDs were used to measure the  $\alpha$ -particles' energy and direction while the  $\beta$ 's were detected by the SDs. The majority of  $\beta$  particles from the  $^8\text{Li}$  decay are too energetic to have been stopped in the SDs and therefore only the momentum directions were obtained. Knowing the two  $\alpha$ -particle momenta and the  $\beta$  direction determines the entire  $^8\text{Li}$  decay kinematics. The pulses from all strips of the four DSSDs and the SDs were recorded whenever a signal on any strip of the DSSD rose above the threshold. The requirement of triple coincidence of two  $\alpha$ -particle signals on opposite DSSDs and a  $\beta$  particle detected in an SD essentially suppressed all background. The DSSDs were continually calibrated *in situ* using  $^{148}\text{Gd}$  and  $^{244}\text{Cm}$  sources that provided  $\alpha$  particles at energies of 3182.690(24) and 5804.77(5) keV, respectively [31].

The time relative to the loading and ejecting of the ions was also recorded to enable selection of decays that occurred after the ions were cooled. The ion cooling process and the ion cloud properties could be monitored by the strip distribution of the two  $\alpha$  particles on opposite DSSDs. The front and back side strips allowed an independent analysis along the axial direction confined by a dc potential and in the radial directions confined by an rf field. The time

dependence of the  $\alpha$ - $\alpha$  correlation indicated that after 20 ms the ion cloud had reached its final size which could be approximated by a Gaussian distribution with 1.8 mm FWHM in all three directions, with an ion temperature of  $< 0.1$  eV [29] which is negligible compared to the several keV recoil  $^8\text{Be}^*$  kinetic energy. The observed decay rate of the trapped  $^8\text{Li}$  ions was consistent (within the 15% measurement uncertainty) with the known 840-ms  $^8\text{Li}$  half-life, indicating that most of the captured  $^8\text{Li}$  ions remain trapped until decay.

Data were collected for 20 h and about 20000  $\alpha$ - $\alpha$ - $\beta$  coincidence events were recorded. The observable most sensitive to a tensor interaction contribution is the  $\alpha$ -particle energy difference spectrum when the  $\beta$  and  $\alpha$  particles are parallel. Events were selected for analysis if (1) the ions had been loaded in the trap for more than 20 ms, which is the time required to thermalize the ions, and (2) the  $\alpha$ -particle energies measured by the front and back side of the DSSD agreed to within 10%; otherwise this would indicate a hit in the gap between adjacent strips, known as the gap effect [32].

A comparison of the  $\alpha$ -particle energy difference spectrum obtained from the top-bottom detector pair and the simulated spectra for a pure axial-vector and a pure tensor interaction is shown in Fig. 2. The Monte Carlo simulations are adapted from the  $\beta$ -decay event generation code used in Refs. [8,33] with the population of the broad  $^8\text{Be}^*$  final state from Ref. [34], and further included the GEANT4 [35] toolkit to simulate the particle interactions with matter. The event generation is based on Eq. (3), with the recoil-order terms of order  $E_e/M_{\text{Li}}$  and the order- $\alpha$   $Z$ -dependent [15] and  $Z$ -independent [36] radiative corrections included. The order- $\alpha$  radiative corrections are dominated by the  $Z$ -independent corrections. The recoil-order terms and

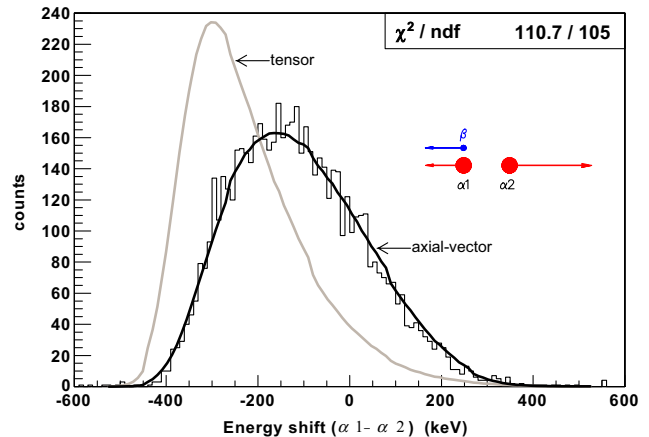


FIG. 2 (color online).  $\alpha$ -particle energy difference spectrum obtained from the top and bottom DSSDs, with  $\beta$  particles detected by the top or bottom SD. The gray curve is the line shape for a pure tensor interaction and the black curve is the line shape for a pure axial-vector interaction. The value of the chi-squared per number of degrees of freedom ( $\chi^2/\text{ndf}$ ) is shown in the text box.

radiative corrections contribute a few percent corrections to these angular-correlation parameters.

The simulation includes the geometry of the experimental setup, the ion cloud distribution, the  $\beta$  scattering, and the detector response. The energy loss in the detector dead layer is accounted for event by event in the determination of the  $\alpha$ -particle energies. Effects due to the rf field, the helium buffer gas, and the finite ion temperature are negligible.

The only free parameter in the fits is the relative intensities of the coupling constants  $|C_T/C_A|^2$ . From the spectrum shown in Fig. 2 obtained from the top-bottom pair, the permissible amount of tensor admixture is determined to be  $|C_T/C_A|^2 = 0.004 \pm 0.012_{\text{stat}}$ , where the  $1\sigma$  uncertainty here is due to statistics alone. A similar but slightly less precise result,  $|C_T/C_A|^2 = 0.003 \pm 0.014_{\text{stat}}$ , was obtained from the energy difference spectrum generated from the left-right detectors. These results are not sensitive to the fitting region selected.

Table I lists the major systematic uncertainties, determined by varying each parameter within its  $1\sigma$  uncertainty range. Each item is independent; therefore, the total systematic uncertainty is the square root of the quadratic sum of the individual contributions.

*Beta scattering.*—A GEANT4 simulation of the trap and detectors indicates that about 8% of the  $\alpha$ - $\alpha$ - $\beta$  coincidences resulted from scattered  $\beta$  particles that otherwise would not have been detected. Most of this scattering is by material close to the detectors. The overall  $\beta$  scattering effects contribute a 0.02 correction to the fit result. The GEANT4 simulation is estimated to have a 15% uncertainty in the electron scattering [37] which introduces a  $0.15 \times 0.02 = 0.003$  uncertainty in this correction.

*Ion cloud distribution.*—Varying the ion-cloud distributions from a Gaussian distribution with FWHM between 0–1.8 mm to a uniform distribution or to a two-peaked distribution suggested in Ref. [38] changes the fit results by  $\leq 0.003$ .

*DSSD energy calibration.*—The energy difference spectrum is dependent on the DSSD energy calibrations. The calibration sources were not specifically made to be very thin, which made the energy calibration more difficult. Some  $\alpha$  particles lose energy when passing through the source material, broadening the low-energy slope of the

energy spectrum. The high-energy falloff of the spectrum remains sharp because the  $\alpha$  particles emitted from the source surface emerge with their full energy. The halfway points on the high-energy side of the  $^{148}\text{Gd}$  and  $^{244}\text{Cm}$  peaks served as secondary standards to monitor the gain and offset of each detector element. The energy of these points was accurately determined off-line by comparison with spectra obtained from thin  $\alpha$  sources. The uncertainty in the energies of the calibration points was determined to be less than 5 keV.

*Detector dead layer.*—The  $\alpha$ -particle energy losses in the dead layers of the DSSDs were measured by placing an  $\alpha$  source at different angles relative to the detector surface. From the energy loss rate ( $dE/dx$ ) calculated using the SRIM program [39], the dead layer thicknesses for the top, bottom, left, and right detectors were determined to be  $0.62 \pm 0.05$ ,  $0.60 \pm 0.05$ ,  $0.60 \pm 0.10$ ,  $0.60 \pm 0.10$   $\mu\text{m}$ , respectively. The energy lost in these dead layers by each of the two  $\alpha$  particles following  $^8\text{Li}$  decay was determined based on the incident angle. The dead layer uncertainties are mainly limited by statistics and therefore should be at least partially uncorrelated. However, to be conservative, they were treated as correlated, which results in an overall systematic uncertainty of 0.006.

*$\beta$ - $\alpha$  summing in the DSSDs.*—The  $\beta$  particles deposited on average only about 90 keV in the DSSDs and they were not well separated from the background. However, on a  $16 \times 16$  DSSD, there is only about a 1/16 chance that the  $\beta$  particle will hit the same strip that the  $\alpha$  particle hit. Therefore, on average, the  $\alpha$ -particle energy difference is decreased by about 5 keV because the  $\beta$  particle more frequently strikes the same detector as the lower energy  $\alpha$  particle. This effect is included in the simulations, but taking into account the 15% uncertainty of the GEANT4 simulation, this effect gives an uncertainty of 0.004 on the value of  $|C_T/C_A|^2$ .

Combining the results from both sets of detectors and including the systematic uncertainties gives:

$$|C_T/C_A|^2 = 0.004 \pm 0.009_{\text{stat}} \pm 0.010_{\text{syst}},$$

with the uncertainties quoted at  $1\sigma$ . The tensor contribution is therefore constrained to  $|C_T/C_A|^2 \leq 0.031$ , and the relative strength of tensor and axial-vector coupling constants is limited to  $|C_T/C_A| \leq 0.18$  (both at 95.5% C.L.), consistent with the standard model description of the electroweak interaction. For comparison with previous experiments, from the above  $|C_T/C_A|^2$  the (allowed order)  $\beta$ - $\bar{\nu}$  angular correlation coefficient  $a_{\beta\nu} = -0.3307 \pm 0.0060_{\text{stat}} \pm 0.0067_{\text{syst}}$  and the triple correlation coefficient  $g_{12}/g_1 = -0.992 \pm 0.018_{\text{stat}} \pm 0.020_{\text{syst}}$  (at  $1\sigma$ ) are calculated and agree with the standard model predictions of  $-1/3$  and  $-1$ , respectively. Thus, the present result on a different system with very different systematic effects agrees with the long-standing result of the  $^6\text{He}$  decay measurement by Johnson *et al.* [4]. Note that a  $1\sigma$

TABLE I. Dominant sources of systematic uncertainties, quoted at  $1\sigma$ .

Source	Uncertainty	$\Delta C_T/C_A ^2$
$\beta$ scattering	15%	0.003
Ion cloud distribution	See text	0.003
DSSD energy calibration	5 keV	0.005
Detector dead layer	0.05–0.10 $\mu\text{m}$	0.006
$\beta$ - $\alpha$ summing in DSSDs	15%	0.004
Total		0.010



uncertainty of 0.0135 in  $|C_T/C_A|^2$  is obtained from a 2.7% measurement of the correlation coefficients because of the relationships in Eqs. (2) and (4). If the restriction on the nature of the tensor interactions (i.e., that  $C_T = -C'_T$ ) is relaxed, the result for  $|C_T/C_A|^2$  becomes a constraint on  $(|C_T|^2 + |C'_T|^2)/(2|C_A|^2)$ .

In this work, a stringent limit on the tensor interaction is achieved with limited statistics by studying the  $\beta$  decay of  $^8\text{Li}$ . The additional  $\alpha$ - $\beta$ - $\bar{\nu}$  correlation and large energy shift in the delayed  $\alpha$ -particle emission make  $^8\text{Li}$  an appealing candidate for higher precision tests of the standard model. It is expected that with an upgraded detector system and much better statistics the limit  $|C_T/C_A|^2$  can be improved by an order of magnitude and precision measurements of recoil-order terms sensitive to the conserved-vector-current hypothesis and second-class currents can be performed.

We acknowledge the ATLAS staff and thank Dariusz Seweryniak for lending us electronics. This work was carried out under the auspices of the NSERC, Canada, Application No. 216974, and the U.S. Department of Energy, by Argonne National Laboratory under Contract No. DE-AC02-06CH11357, by Northwestern University under Contract No. DE-FG02-98ER41086, and Lawrence Livermore National Laboratory under Contract No. DE-AC52-07NA27344.

- 
- [1] E.D. Commins, *Weak Interactions* (McGraw-Hill, New York, 1973).
- [2] N. Severijns, M. Beck, and O. Naviliat-Cuncic, *Rev. Mod. Phys.* **78**, 991 (2006).
- [3] P. Herczeg, *Prog. Part. Nucl. Phys.* **46**, 413 (2001).
- [4] C.H. Johnson, F. Pleasonton, and T.A. Carlson, *Phys. Rev.* **132**, 1149 (1963).
- [5] F. Glück, *Nucl. Phys.* **A628**, 493 (1998).
- [6] X. Fléchar, Ph. Velten, E. Liénard, A. Méry, D. Rodríguez, G. Ban, D. Durand, F. Mauger, O. Naviliat-Cuncic, and J.C. Thomas, *J. Phys. G* **38**, 055101 (2011).
- [7] A. Gorelov *et al.*, *Phys. Rev. Lett.* **94**, 142501 (2005).
- [8] P.A. Vetter, J.R. Abo-Shaeer, S.J. Freedman, and R. Maruyama, *Phys. Rev. C* **77**, 035502 (2008).
- [9] A. Knecht *et al.*, *APS Meeting Abstracts* (Bulletin of the American Physical Society, Anaheim, California, 2011), Vol. 56, p. 99.
- [10] M. Simson *et al.*, *Nucl. Instrum. Methods Phys. Res., Sect. A* **611**, 203 (2009).
- [11] E.K. Warburton, *Phys. Rev. C* **33**, 303 (1986).
- [12] W.T. Winter, S.J. Freedman, K.E. Rehm, and J.P. Schiffer, *Phys. Rev. C* **73**, 025503 (2006).
- [13] R. Wiringa (private communication).
- [14] M. Morita, *Phys. Rev. Lett.* **1**, 112 (1958).
- [15] B.R. Holstein, *Rev. Mod. Phys.* **46**, 789 (1974).
- [16] K. Siegbahn, *Alpha- Beta- and Gamma-Ray Spectroscopy* (North-Holland, Amsterdam, 1965).
- [17] E.G. Adelberger, C. Ortiz, A. García, H. E. Swanson, M. Beck, O. Tengblad, M.J.G. Borge, I. Martel, and H. Bichsel, *Phys. Rev. Lett.* **83**, 1299 (1999).
- [18] E.T.H. Clifford *et al.*, *Phys. Rev. Lett.* **50**, 23 (1983).
- [19] V. Vorobel *et al.*, *Eur. Phys. J. A* **16**, 139 (2003).
- [20] V. Egorov *et al.*, *Nucl. Phys.* **A621**, 745 (1997).
- [21] J.D. Jackson, S.B. Treiman, and H.W. Wyld, *Phys. Rev.* **106**, 517 (1957).
- [22] A.S. Carnoy, J. Deutsch, T.A. Girard, and R. Prieels, *Phys. Rev. C* **43**, 2825 (1991).
- [23] B.R. Holstein, *Phys. Rev. C* **16**, 753 (1977).
- [24] T. Sumikama *et al.*, *Phys. Rev. C* **83**, 065501 (2011).
- [25] L. Grenacs, *Annu. Rev. Nucl. Part. Sci.* **35**, 455 (1985).
- [26] T. Sumikama *et al.*, *AIP Conf. Proc.* **915**, 230 (2007).
- [27] G. Savard *et al.*, *Nucl. Instrum. Methods Phys. Res., Sect. B* **204**, 582 (2003).
- [28] J. Fallis, Ph.D. thesis, University of Manitoba, 2009.
- [29] N.D. Scielzo *et al.*, *Nucl. Instrum. Methods Phys. Res., Sect. A* **681**, 94 (2012).
- [30] G. Savard, St. Becker, G. Bollen, H.-J. Kluge, R.B. Moore, Th. Otto, L. Schweikhard, H. Stolzenberg, and U. Wiess, *Phys. Lett. A* **158**, 247 (1991).
- [31] NUDAT 2.6, Brookhaven National Laboratory, <http://www.nndc.bnl.gov/nudat2/>.
- [32] J. Yorkston, A.C. Shotton, D.B. Syme, and G. Huxtable, *Nucl. Instrum. Methods Phys. Res., Sect. A* **262**, 353 (1987).
- [33] N.D. Scielzo, S.J. Freedman, B.K. Fujikawa, and P.A. Vetter, *Phys. Rev. Lett.* **93**, 102501 (2004).
- [34] M. Bhattacharya, E.G. Adelberger, and H.E. Swanson, *Phys. Rev. C* **73**, 055802 (2006).
- [35] GEANT4, <http://geant4.web.cern.ch/geant4>.
- [36] F. Glück, *Comput. Phys. Commun.* **101**, 223 (1997).
- [37] S.A. Hoedl, Ph.D. thesis, Princeton University, 2003.
- [38] J. Hou, Y. Wang, and D. Yang, *J. Appl. Phys.* **88**, 4334 (2000).
- [39] SRIM, <http://www.srim.org/#SRIM>.